SLAC–PUB–6452
February 1994
(M)

Gas Bremsstrahlung Considerations in the Shielding Design of the Advanced Photon Source Synchrotron Radiation Beam Lines*

Nisy E. Ipe

Radiation Physics Department

Stanford Linear Accelerator Center

Stanford University, Stanford, California 94309

(415) 926-4324

Alberto Fassò

TIS / RP CERN CH–1211

Geneve 23

Switzerland

(41) 22 767 3937

Abstract

The Advanced Photon Source (APS) currently under construction at Argonne National Laboratory will be one of the world's brightest synchrotron radiation (SR) facilities. The storage ring, capable of storing currents up to 300 mA at 7.0 GeV, or 200 mA at 7.5 GeV, will produce very intense and energetic synchrotron radiation (E_C = 24 keV for bending magnets, and E_C = 37.4 keV for wigglers, where E_C is the critical energy). The synchrotron radiation beam

* Work supported by Department of Energy contract DE–AC03–76SF00515.
Submitted to Nuclear Instruments and Methods A

lines, consisting of experimental enclosures and transport lines, will have to be shielded against synchrotron radiation and gas bremsstrahlung scattered from beam line components. For insertion devices placed in the straight sections (length = 15 m), the gas bremsstrahlung produced by the interaction of the primary stored beam with residual gas molecules or ions in the storage ring vacuum chamber dominates the SR beam line shielding. Gas bremsstrahlung in the forward direction will be stopped by a tungsten beam stop, 18 cm thick, located at the back of the experimental enclosure and placed in the median plane of the storage ring. The forward-directed gas bremsstrahlung is characterized, and the effectiveness of the tungsten beam stop is assessed. The Monte Carlo code FLUKA was used to determine the dose equivalent rates from gas bremsstrahlung in a cylindrical tissue phantom with and without the tungsten beam stop. Simulations were performed using an air target of length 15 m at a pressure of 1 atm and 1/10 atm (1 atm = 101.325 kPa = 760 torr) both with and without suppressing positron multiple scattering (M.S.) and Bhabha and Moller scattering in the air target. At a given pressure the dose equivalent rates are higher without positron multiple scattering in the air target than with multiple scattering. For simulations at Ps = 1 atm, the minimization of Bhabha/Moller scattering is important for areas with scoring radii less than 0.4 cm. The maximum dose equivalent rate (for E_0 = 7 Gev, I = 300 mA, and P = 0.133 μPa or 10^{-9} torr) in the phantom (at a depth of 29.5 cm) for a scoring area of 0.0013 cm^2 (radius = 0.02 cm) is 2.1 Sv/h, whereas for a scoring area of 0.5 cm^2 (radius = 0.4 cm) it is 0.57 Sv/h. Scoring photon fluence and converting it to dose equivalent using Rogers' fluence-to-dose equivalent conversion factors results in an overestimation of dose equivalent. The

maximum dose equivalent rate behind the tungsten beam stop, at a depth of 2.5 cm in the tissue, is 0.1 + 0.04 μSv/h for a scoring radius of 1 cm. The corresponding dose equivalent rates without the stop are 32 mSv/h (depth = 2.5 cm) and 0.17 Sv/h (depth = 29.5 cm). A simple expression has been derived for the upper limit on the dose equivalent that an individual can receive due to loss of vacuum in the straight section.

1. Introduction

The Advanced Photon Source (APS) currently under construction at Argonne National Laboratory, Illinois will be one of the world's brightest synchrotron radiation facilities [1]. The machine is composed of an electron linear accelerator (linac), a positron linac, a positron accumulator ring (PAR), a booster synchrotron injector, and a storage ring (fig. 1). Electrons produced by an electron gun will be accelerated to 200 MeV in the linac and allowed to strike a target, producing electron-positron pairs. The positrons will be captured, focused, and accelerated to 450 MeV, and then accumulated in the PAR, from which they will be transported to the booster synchrotron which will raise their energy to 7 (or 7.5) GeV. The positrons (7.2×10^{10} e^+/s) will then be injected into the storage ring (circumference = 1104 m), which is capable of storing circulating currents up to 300 mA at 7.0 GeV, or 200 mA at 7.5 GeV.

Special bending magnets and focusing magnets will guide the beam as the positrons move at nearly the speed of light around the circular storage ring maintained at a vacuum of 0.133–0.0133 μPa (10^{-9}–10^{-10} torr). The positrons

radiate energy (synchrotron radiation) as they are being deflected in the fields of storage ring bending magnets (BMs) or special magnets called insertion devices (IDs) which are placed in the straight sections (of length, L = 15 m) of the storage ring. The synchrotron radiation (SR) is polarized, very highly collimated, and extremely intense.

An ID consists of a series of short magnets with alternating magnetic fields (fig. 1), which cause the particles either to wiggle or undulate as they pass through the device. Since the positrons are forced to change direction many times in a short distance, the brightness (number of photons per second per unit solid angle per unit source area) is greatly enhanced. Wigglers produce very intense, energetic radiation over a wide range of x-ray energies, while undulators yield radiation of selected energy with high brightness. Sixty-eight SR beam lines, half originating at BMs and the other half at IDs, will be transported to the Experimental Floor through penetrations in the ratchet-shaped storage ring shielding walls. The portion of the SR beam line within the storage ring is referred to as the front end (fig. 2).

A typical APS SR beam line will consist of a first-optics enclosure (FOE), a white beam hutch (WBH), a beam transport line (BTL) and a monochromatic beam hutch (MBH) (fig. 2). The entire SR spectrum, known as the white beam, can be transported to the WBH, or if desired a monochromator can be used in the FOE, and a monochromatic (mono) beam can be transported to the MBH for experimental purposes. Mirrors may sometimes be used in the FOE to obtain “pink beam” (reflected white light).

Photons and neutrons produced by the interaction of the primary injected or stored positron beam with the storage ring components may be of concern on the Experimental Floor during normal or abnormal beam operating conditions. Protection is achieved through the adequate design of the storage ring shielding wall and the use of local shielding. In addition, the front-end photon shutter and two safety shutters (fig. 2) are closed during operation. The photon shutter and stop are water-cooled and absorb most of the synchrotron radiation heat load, while the safety shutters, made of tungsten of thickness 30 cm each, and the safety stop (18 cm of tungsten) provide protection in the forward direction from gas bremsstrahlung, white beam, and radiation from beam losses in the storage ring.

Gas bremsstrahlung is produced by the interaction of the primary stored beam with residual gas molecules (H_2, CO, CO_2, CH_4, etc.) or ions in the storage ring vacuum chamber. It is produced in a narrow cone, the characteristic emission angle being given by $1/\gamma$, where $\gamma = E_0 / m_0c^2$ (E_0 = primary beam energy and m_0c^2 = rest mass energy of electron/positron). As E_0 increases the characteristic emission angle decreases, and the gas bremsstrahlung becomes more forward peaked. The bremsstrahlung spectrum of photons extends up to the energy of the primary beam.

Gas bremsstrahlung becomes very important for straight sections in the storage ring, since the contribution from each interaction adds up to produce a narrow monodirectional beam which travels down the SR beam line along with the synchrotron radiation. Both gas bremsstrahlung and synchrotron radiation can scatter off any beam line component they strike (mirrors, slits,

masks, shutters, monochromators, etc.). The gas bremsstrahlung can develop an electromagnetic shower in any target it strikes. In addition, gas bremsstrahlung can produce neutrons in any target. Photoneutrons are produced when the photon energy is greater than the threshold for photo-neutron production. Scattered gas bremsstrahlung requires far greater shielding thicknesses than scattered synchrotron radiation.

According to Ferrari et al. [2], the maximum gas bremsstrahlung dose rate D (Gy / h) in the forward direction (for energies ranging from 100 MeV to 1 GeV and straight section lengths of 1 to 50 m), based on Monte Carlo calculations, is given by

$$\dot{D} = 2.5 \times 10^{-27} \left(\frac{E_0}{m_0 c^2} \right)^{2.67} \frac{L}{d(L+d)} I \frac{P}{P_0}, \qquad (1)$$

where E_0 is the primary beam energy (MeV); m_0c^2 is the rest-mass energy of the electron / positron (MeV); L is the length of the straight section (m); d is the distance from the end of the straight section to the point of interest (m); I is the stored beam current (e^- / s); P is the pressure in the straight section (Pa); and P_0 = 1.33 x 10^{-7} Pa (10^{-9} torr). Since gas bremsstrahlung becomes more forward peaked as the primary beam energy increases, this expression was derived using different scoring areas at different energies. For E_0 > 500 MeV, a scoring area of 0.0059 cm^2 was used.

Using the above expression (assuming that it is still valid at 7.0 GeV), the gas bremsstrahlung dose rate for E_0 = 7.0 GeV, I = 300 mA, P = 1.33 x 10^{-7} Pa, L = 15 m, and d = 32.6 m is 5 Sv / h. The ratio of the gas bremsstrahlung dose rates at a given pressure for d = 20 m are shown in Table 1 for the APS, the ESRF

(European Synchrotron Radiation Facility), and SSRL (Stanford Synchrotron Radiation Facility). The gas bremsstrahlung dose rate in the forward direction for the APS will be 61 times higher than that for SSRL. This implies that scattered gas bremsstrahlung dose rates will also be much higher for the APS than for SSRL.

At most of the existing synchrotron radiation facilities, such as SSRL, gas bremsstrahlung in the forward direction is shielded by safety stops placed in the median plane of the primary stored beam and at the back of the experimental enclosure/hutch. The safety stops in the APS will made of tungsten, 18 cm thick. However, the lateral and back walls of most of these facilities have been shielded only for scattered synchrotron radiation. The impacts of scattered synchrotron radiation, scattered gas bremsstrahlung, and neutrons produced by gas bremsstrahlung, on synchrotron beam line shielding are discussed in other papers [1,4]. The gas bremsstrahlung dose rates in the forward direction are discussed in this paper.

2. Shield Design Criteria

The shielding for the SR beam lines is designed to keep the annual integrated dose equivalent at the shield surface in occupied areas to less than 5 mSv. This design criterion is based on DOE recommendations [3]. For a 2000-h operating year this corresponds to 2.5 μSv/h.

3. Simulation of Forward Directed Gas Bremsstrahlung

Several efforts have been made to characterize, quantify, and measure the gas bremsstrahlung produced at electron storage rings [2,5–10]. In the papers in which the results of Monte Carlo calculations have been presented, the authors have scored photon fluence and used fluence to dose equivalent conversion factors to determine the gas bremsstrahlung dose equivalent [2,5–10]. The actual energy deposited in tissue by gas bremsstrahlung was not determined. In this paper we present the results of energy deposition and results using fluence to dose equivalent conversion factors, which we will show overestimate the dose equivalent. Some of the authors [5,10] mentioned above did not suppress multiple scattering (M.S.) in the air path traversed by the electrons. Multiple scattering broadens the bremsstrahlung beam, thus making it less forward peaked; however, the total number of photons in the beam remains the same. Therefore the dose equivalent rates in a given scoring area will be lower with multiple scattering turned on, than with multiple scattering suppressed. This will lead to an underestimation in dose equivalent as was pointed out by Ferrari et al. [2]. The consequences of not suppressing multiple scattering in the air path will also be described in this paper.

As described by Ferrari et al. [2], the choice of area over which the gas bremsstrahlung dose rates are determined becomes very important because the dose rates become more forward peaked with increasing E_0. Averaging over large areas results in underestimation of dose. As the areas are made smaller, the Monte Carlo statistics become poorer. The area must be optimized

so that it is small enough to avoid underestimation but large enough to save computer time.

The calculations presented here were performed only for the straight sections of the storage ring because the gas bremsstrahlung from the bending magnet is reduced significantly by the much shorter effective straight section seen by the SR beam line. The beam is spread over a larger area as compared to the ID [8].

The FLUKA program was used to determine the production of gas bremsstrahlung. The most recent version of the code [11,12] includes a complete treatment of electron/positron and photon interactions at all energies above 1 keV and, in particular, an accurate description of bremsstrahlung angular distributions. Since the residual pressure P in the storage ring is very low (0.133 to 0.0133 μPa), in the simulation the straight section (L = 15m) was represented by an air target at atmospheric pressure (101.325 kPa), and the results were later scaled to 0.133 μPa. In order to avoid confusion, hereafter the pressure at which the simulation is carried out will be referred to as the simulation pressure (P_s), and the pressure to which the results are scaled will be referred to as the pressure P. The equivalence of air and the residual gas in terms of average atomic numbers has been established, although the chemical composition differs [5].

A pencil beam of positrons (E_0 = 7.0 GeV) was allowed to strike the air target. In reality the beam profile will have a Gaussian shape; therefore the gas bremsstrahlung dose equivalent rates will be slightly lower than for the pencil beam case.

The interaction probability per positron would be extremely low at the actual pressure of the residual gas (0.133 to 0.0133 μPa). As long as the positron interaction probability is kept smaller than a few percent, self-absorption in the air target can be neglected. As discussed by Ferrari et al. [2], the calculated results can be scaled to the actual pressure value, provided that all interactions except bremsstrahlung are suppressed or at least minimized. Therefore, no positron multiple scattering was allowed in the air target. Positrons bending in the fields of the storage ring magnets were accounted for by removing them at the downstream end of the air target (killing region) since they will not travel down the SR beam line.

The bremsstrahlung beam was transported through vacuum (representing the vacuum in the beam pipe) until it struck the base of a cylindrical phantom of ICRU tissue (enclosed in vacuum) located 32.6 m from the start of the straight section. The tissue phantom (radius = 20 cm, length = 30 cm) was divided into 30 regions, each of thickness 1 cm. The energy deposited in radial bins 0.02 cm wide from r = 0 to r = 0.4 cm, and in radial bins 1 cm wide from r = 0 to r = 20 cm in each region and the photon fluence crossing the surfaces of volume elements of different radii were scored. The calculations were also performed without suppressing the positron multiple scattering in the air path. Ferrari et al. [2] have recommended that for long straight sections (> 10 m) the simulation should be carried out at 1/10 of the atmospheric pressure (instead of at atmospheric pressure) because the distribution of interactions in the long straight section will differ at the two pressures. Hence, the simulations were repeated at P_S = 1/10 atm. The simulations were also repeated for a single

radial bin of width 0.043 cm corresponding to an area of 0.0059 cm^2 in order to compare our results with eq. 1.

The positron/electron (C_e) and photon (C_p) cut-offs for the different media were as follows: Air (target) C_e = 10 MeV, C_p = 1.0 keV; Air (killing region) C_e = 7.0 GeV, C_p = 1.0 keV; Air (intervening) C_e = 10 keV, C_p = 1.0 keV; and Tissue C_e = 10 keV, C_p = 1.0 keV The calculations were also repeated by changing the AE to 10 MeV from 10 keV for the air target (AE is the lower energy cut-off in the material for charged particle transport and is the energy threshold below which electron interactions are taken to be continuous. Secondary particles with energy above AE are produced in a discrete way, that is, delta rays and bremsstrahlung).

The calculations were then performed at P_s = 1/10 atm with the introduction of a tungsten beam stop ($20 \times 20 \times 18$ $cm^{3)}$ in front of the tissue phantom, located 32.1 m from the start of the straight section. Leakage from the sides of the stop was eliminated by surrounding the stop laterally with a black hole. Since the stop is fairly thick, it presents a deep penetration problem, that is, one in which the sample sizes with straight Monte Carlo becomes increasingly small with depth [13]. Only a small fraction of the photons might penetrate the stop, providing a statistically poor picture of the energy and angular distribution of the photons emerging from the stop. Therefore, the stop was divided into eighteen 1-cm-thick regions. The number of photons (using leading particle biasing) crossing the boundary of each region was scored. Leading particle biasing means that at each interaction only one of the two particles leaving the collision is followed. The probability of each of the

particles to be selected is proportional to its useful energy. The weight of the particle is adjusted by multiplying by the inverse of the selection probability.

The data obtained with the leading particle biasing were then used as a guide to set region parameters for a more efficient variance reduction technique based on Russian Roulette and splitting at the boundaries.

This can be done with FLUKA in several ways: the option chosen was the simplest one, in which the number of particles entering a given region is reduced or increased by a factor equal to the ratio of the region “importances” on either side of the boundary. Importances are region dependent parameters which can be tuned by the user in order to control the sample size in different parts of the geometry. Of course, the code automatically ensures that total particle weight is conserved. Each of the 18 regions in tungsten was assigned an importance inversely proportional to the expected number of photons at the corresponding depth, so as to obtain an approximately uniform photon population throughout the whole block. No biasing was applied at the tungsten tissue surface. The energy deposited in each 1-cm thick region was also scored.

The positron/electron (C_e) and photon (C_p) cut-offs for tungsten were as follows: Regions 1–16 C_e = 5.0 MeV, C_p = 10 keV; Region 17 C_e = 1.0 MeV, C_p = 1.0 keV ; Region 18 C_e = 10 keV, C_p = 1.0 keV; and Tissue C_e = 10 keV, C_p = 1.0 keV (AE for air target = 10 MeV).

In the next section the average values and standard deviations of the results for five runs (for I = 300 mA and P = 0.133 μPa with positron multiple

scattering suppressed in the air target) are reported for P_S = 1/10 atm (~61,000 particles followed per run), and P_S = 1 atm (~40,000 particles followed per run) with AE for air target = 10 keV. Only one run each was performed for all the other simulations. The numbers of particles were approximately 67,000 and 63,000 for simulations with positron multiple scattering turned on for P_S = 1/10 and P_S = 1 atm, respectively. Only one run was performed with AE = 10 MeV for Ps = 1/10 (~558,000 particles) and Ps = 1 atm (61,000 particles) with multiple scattering suppressed and one run without suppressing multiple scattering. (Ps = 1/10 ~550,000 particles and Ps = 1 atm ~62,000 particles). Five runs were performed with the tungsten stop placed upstream of the tissue phantom (~ 135,000 particles/run).

The "average" dose equivalent rates were obtained by scoring the energy deposition in 1-cm-thick regions of tissue and averaging over surfaces of different radii. The "maximum" dose equivalent rates were obtained by multiplying the photon fluence rates by the maximum fluence to dose equivalent conversion factors published by Rogers [14]. These factors are the maximum dose equivalent per unit fluence for broad parallel beams of monoenergetic photons incident on a 30-cm-thick slab of ICRU tissue. The gas bremsstrahlung beam is a narrow beam consisting of a spectrum of photons. Furthermore, the true maximum dose equivalent for each energy occurs at a different depth in the tissue. Therefore the applicability of Rogers' conversion factors in this situation is in question, as it will overestimate the dose equivalent. As discussed before, several authors have used these conversion factors.

Error bars are shown only for the cases in which five runs were performed. Error bars less than a few percent are not visible in the figures.

Results and Discussion

Figure 3 shows the differential photon spectra (where the photon fluence is expressed as photons per cm^2 per MeV per positron) crossing the tissue surface (r = 20 cm, AE for air target = 10 keV) for $P_s = 1$ and $P_s = 1/10$ atm, scaled to P = 1 atm. The error bars for $P_s = 1/10$ atm are less than a few percent and are therefore not visible in the figure. The attenuation of the low-energy photons (< 100 keV) at 1 atm is clearly visible. Also shown is the photon spectra scaled to P = 1 atm without suppressing multiple scattering (in air) for $P_s = 1/10$ atm. There is no significant difference in the spectra with and without multiple scattering. The results for calculations performed with AE for the air target = 10 MeV were identical to those obtained with AE = 10 keV for Ps = 1 and 1/10 atm, respectively.

Figure 4 shows the "average" dose equivalent rate for $P_s = 1/10$ atm (E_0 = 7 GeV, I = 300 mA, and P = 0.133 μPa, AE for air target = 10 keV), as a function of depth in tissue for a scoring area with radius r = 0.02 cm. This was the smallest optimum scoring area (0.0013 $cm^{2)}$ that could be used. Also shown are the results for r = 0.4 cm. As the radius increases the dose equivalent rate decreases. In general, the dose equivalent rate increases with depth and reaches a maximum at the back of the tissue phantom. The "average" dose equivalent rates at a depth of 29.5 cm is 1.61 ± 0.04 Sv/h and 0.56 ± 0.004 for

r = 0.02 cm and 0.4 cm, respectively. The corresponding "maximum" dose equivalent rate for r = 0.02 cm (using Rogers' conversion factors) is 6.36 Sv / h .

Ferrari's [2] equation for an area of 0.0059 cm^2 (r = 0.043 cm) yields 5 Sv / h. Our calculations for the same area yield 1.57 ± 0.03 and 6.1 Sv / h for the "average" and "maximum" dose equivalent rates, respectively. These results are not very different from the results at r = 0.02 cm. Since Ferrari's equation has been derived for energies up to 1 GeV, using it at 7 GeV is an extrapolation which leads to some uncertainty. Furthermore, the procedure of converting fluence to dose equivalent carries some uncertainty, mainly due to the way the interpolation is carried out (linear, logarithmic, bin structure, number of points per bin, etc.). Under these circumstances, the agreement between the two numbers is fairly reasonable. However, use of the "maximum" dose equivalent rate clearly results in an overestimation of the dose equivalent rate, in this case by a factor of about 4. Interestingly enough Ferrari et al. [2] have reported measurements for the Adone ring which indicate that the calculated values overestimate the measured values by about a factor of 3.7. The maximum "average" dose equivalent for Ps = 1 atm is 0.8 Sv / h (not shown) which is about a factor of 2 lower than at Ps = 1 / 10 atm. This difference can be attributed to the fact that when AE = 10 keV, delta rays above 10 keV are produced and even though they are not transported (C_e for air target = 10 MeV) they deflect the primary positron or electron beam (Bhaba and Moller scattering) which broadens the beam. The thresholds for discrete Bhabha and Moller scattering are AE and 2AE – $m_o c^2$, respectively. Raising AE is therefore equivalent to raising the thresholds for discrete Bhabha and Moller scattering, which in turn reduces Bhabha and Moller scattering.

Bhabha and Moller scattering increase as the pressure of the air target increases. The simulations were repeated with AE for the air target raised to 10 MeV for both Ps = 1 and 1/10 atm and the results are shown in fig. 5.

There is no significant difference in the dose equivalent rates between Ps = 1/10 and Ps = 1 atm for r = 0.02 cm. The maximum "average" dose equivalent rate obtained at a depth of 29.5 cm in tissue is approximately 2.1 Sv/h. The "maximum" dose equivalent rate (using Roger's conversion factors) is 8.3 Sv/h. These dose equivalent rates are higher than the dose equivalent rates obtained with AE for the air target = 10 keV. As discussed before, raising AE reduces the discrete Bhabha and Moller scattering, thus making the beam more forward peaked. At P_S = 1/10 atm the maximum "average" dose equivalent rate is 0. 57 Sv/h for r = 0.4 cm, which is very similar to the result obtained with AE = 10 keV. A comparison of figs. 4 and 5 reveals that the dose equivalent rates at r = 0.02 cm, for AE = 10 MeV are slightly higher than the dose equivalent rates for AE = 10 keV at Ps = 1/10 atm. Data not shown in fig. 4 indicate that the dose equivalent rates are significantly higher at P_S = 1 atm for AE = 10 MeV as compared to 10 keV for r = 0.02 cm. The dose equivalent rates are the same at r = 0.4 cm for AE = 10 keV and 10 MeV at P_S = 1/10 atm, and P_S = 1 atm. The impact of discrete Bhabha and Moller scattering becomes important only when dose equivalent rates are scored over areas with radii smaller than 0.4 cm and is more significant for simulations performed at P_S = 1 atm.

Figure 6 shows the "average" dose equivalent rate for r = 0.4 cm at P_s = 1/10 and P_s = 1.0 atm, with and without the suppression of multiple scattering (AE

of air target = 10 MeV). At a depth of 29.5 cm in tissue, the dose equivalent rates without multiple scattering are factors of 1.2 and 3.5 times higher than the data with multiple scattering at $P_S = 1/10$ and 1 atm, respectively. This is because multiple scattering broadens the bremsstrahlung beam, thus making it less forward peaked. The differences between the results with and without multiple scattering are more significant at $P_S = 1$ atm than at $P_S = 1/10$ atm because there is more multiple scattering with increasing pressure.

Figure 7 shows the "average" dose equivalent rate as a function of maximum radius of integration at a depth of 29.5 cm in the tissue phantom for $P_S = 1/10$ and 1.0 atm with and without multiple scattering (AE = 10 MeV). There are differences of factors of about 3.2 and 6.4 in dose equivalent rates at Ps = 1/10 and 1 atm, respectively, when the radius of the scoring area is 0.02 cm, and about 3.0 and 9.6 for r = 0.4 cm , between the results obtained with and without suppressing multiple scattering. For radii greater than 0.1 cm, as the scoring radius increases, the difference between the results obtained with and without the suppression of multiple scattering, decreases. For radii greater than 0.4 cm the dose equivalent rates with and without multiple scattering approach each other as shown in fig. 8.

For $P_S = 1.0$ atm with multiple scattering, the dose equivalent rates are fairly independent of the scoring radius for radii from 0.04 cm up to 0.4 cm and are significantly lower than the dose equivalent rates without multiple scattering even at r = 0.4 cm (fig. 7).

For radii greater than 2 cm the dose equivalent rates with and without multiple scattering for both Ps = 1/10 and Ps = 1 atm are nearly the same

(fig 8). The impact of multiple scattering becomes more pronounced for dose equivalent rates scored over areas with radii less than 2 cm for Ps = 1 atm.

Figure 9 shows the number of photons per positron crossing the boundaries between regions at various depths in the tungsten stop (surface area = $20 \times 20\ cm^2$). There is a buildup of photons between 2 and 3 cm due to the electromagnetic shower process occurring within the tungsten stop. The photons are then attenuated within the tungsten stop with an attenuation coefficient of approximately $0.04\ cm^2/gm$, which is the minimum (Compton) attenuation coefficient for tungsten. The shower maximum occurs at a depth t given by:

$$t = 1.01\ (\ln k_o / E_{cr} - 0.5),$$

where t is in radiation lengths, k_o is the maximum photon energy, and E_{cr} is the critical energy for the material. For tungsten, t = 2.22 cm. Results obtained by scoring energy deposition in 1-cm-thick layers of tungsten indicate that the maximum energy deposition occurs at a depth between 2 and 3 cm in the tungsten stop.

The differential photon spectra crossing the tissue surface (radius = 20 cm) with and without the tungsten stop upstream of the tissue phantom are shown in fig. 10. The spectrum of the photons after passing through the tungsten stop is quite different and much softer than the pure gas bremsstrahlung spectrum. The K x-rays in tungsten are also visible ($K\alpha_1$ = 59.32 keV).

Figure 11 shows the “average” dose equivalent rate as a function of radius at depths of 2.5 and 26.5 cm in the tissue phantom with and without the tungsten stop placed upstream of the tissue phantom (E_0 = 7 GeV, I = 300 mA, P = 0.133 μPa, Ps = 1/10 atm, L = 15 m, AE for air target = 10 MeV). The gas bremsstrahlung beam has broadened considerably due to the shower process in the tungsten stop as is evidenced by the fact that the dose rates decrease very slowly with increasing radii at a depth of 2.5 cm and practically independent of radius at a depth of 26.5 cm.

In order to assess the effectiveness of the tungsten beam stop, the “average” dose equivalents for r = 3 and 10 cm are shown as a function of depth, with and without the tungsten stop in fig. 12. The dose equivalent rates reach a maximum within the first few cm (2–3 cm) of the tissue phantom, and not at the back of the phantom as in the case without the tungsten stop, because the spectrum is much softer. The dose equivalent rates with the tungsten stop for r = 3 cm are slightly higher than for r = 10 cm up to a depth of about 24.5 cm; after that point the two dose equivalent rates approach each other. There is a significant difference in dose equivalent rates between r = 3 cm and r = 10 cm without the tungsten stop. Data not shown in this figure indicate that the maximum “average” dose equivalent rate is 0.1 + 0.04 μSv/h at a depth of 2.5 cm in the tungsten stop when scored over a radius of 1 cm. The corresponding dose equivalent rate at the same depth and for the same radius without the tungsten stop is 32 mSv/h. The corresponding dose equivalent rate at a depth of 29.5 cm is 0.17 Sv/h. The “maximum” average dose equivalent rate (at a depth of 29.5 cm) for r = 0.02 cm is 2.1 Sv/h as discussed earlier. In order to assess the effectiveness of the tungsten stop it would be

more appropriate to compare the dose equivalent rates measured by a detector of a given radius with and without the tungsten stop. For instance a detector with r = 3 cm, designed to measure the dose equivalent rate at the back of the tissue phantom (depth = 28.5 cm) will measure approximately 0.012 + 0.008 μSv/h and 25 mSv/h, respectively, and at the surface (depth = 0.5 cm) will measure approximately 0.043 + 0.003 μSv/h and 1.1 mSv/h, respectively.

However, a detector with a smaller radius will measure much higher dose equivalent rates without the tungsten stop, because the gas bremsstrahlung dose equivalent rates are highly peaked in the forward direction. A detector with a larger radius will measure significantly lower dose equivalent rates without the tungsten stop.

In addition to the 18-cm thick tungsten stop, the back walls of the experimental hutches will be made of lead of thickness 5 cm, with provisions for additional lead shielding. Therefore, the dose equivalent rates outside the enclosure will be well below the shield design criterion of 2.5 μSv/h.

It must be noted that any increase in pressure in the straight section will cause a corresponding increase in the gas bremsstrahlung dose equivalent rates. However, the pressure in the storage ring cannot rise indefinitely because the stored beam lifetime decreases with increasing storage ring pressure. A simple expression will be derived for the maximum dose equivalent that an individual could be exposed to when the pressure in the straight section increases above the normal operating pressure of $<P_0>$.

The beam lifetime τ at an average storage ring pressure of <P> is the time taken for the number of stored particles to decay to 1/e of its initial value. It can be related to the lifetime τ_0 at an average pressure of $<P_0>$ by the following expression:

$$\tau = \frac{\tau_0 \langle P_0 \rangle}{\langle P \rangle} \quad . \tag{2}$$

It is possible for the pressure in the straight section to increase up to a certain level without affecting the average pressure in the rest of the storage ring because the vacuums in the various sectors of the storage ring are isolated from each other. If the pressure in the straight section rises to $<P_L>$ while the average pressure in the rest of the storage ring remains at $<P_0>$, the average storage ring pressure <P> may be related to the pressure in the straight section by the following expression:

$$\langle P \rangle = \frac{C-L}{C}\langle P_0 \rangle + \frac{L}{C}\langle P_L \rangle \ , \tag{3}$$

where C is the circumference of the ring, and L is the length of the straight section. Since the dose equivalent rate from gas bremsstrahlung is proportional to the stored current, the dose equivalent rate D at any time t, is given by:

$$\dot{D} = \dot{D}_L \, e^{-t/\tau} \quad . \tag{4}$$

where D_L is the initial dose equivalent rate due to gas bremsstrahlung from the straight section at a pressure $<P_L>$. The integrated dose equivalent D during the time period t is given by :

$$D = \int_0^t \dot{D}\, dt = \int_0^t \dot{D}_L \, e^{-t/\tau} dt = \tau \dot{D}_L \left(1 - e^{-t/\tau}\right) \ . \tag{5}$$

$$D = \tau \dot{D}_L , \qquad \text{when } t >> \tau \tag{6}$$

$$\dot{D}_L = \dot{D}_{0L} \frac{\langle P_L \rangle}{\langle P_0 \rangle} , \tag{7}$$

where $\dot{D}_{0L}$ is the dose equivalent rate at the initial operating pressure of $<P_0>$. Substituting eq. 7 in eq. 6 yields

$$D = \tau \dot{D}_{0L} \frac{\langle P_L \rangle}{\langle P_0 \rangle} \tag{8}$$

and substituting eq. 3 in eq. 8 results in the following expression:

$$D = \tau \dot{D}_{0_L} \left(\frac{C\tau_0}{L\tau} - \frac{C-L}{L} \right) . \tag{9}$$

When $C\tau_0 / L\tau >> C - L/L$, the maximum dose equivalent D_{max} is obtained.

$$D_{max} = \frac{C}{L} \tau_0 \dot{D}_{0_L} , \tag{10}$$

$$D = \tau_0 \dot{D}_{0_L} \qquad \text{when } \tau = \tau_0 . , \tag{11}$$

Thus it has been demonstrated that even though the pressure in the straight section increases, there is an upper limit on the dose equivalent because the beam lifetime decreases with increasing pressure. Since the SR beam lines at the APS will be shielded so that the dose equivalent rate outside the shielding is limited to 2.5 μSv / h, the maximum dose equivalent that an individual can be exposed due to an increase in the straight section pressure is 3.7 mSv (C = 1104 m, L = 15 m, $<P_0>$ = 0.133 μPa, τ_0 = 20 h, and $\dot{D}_{0L}$ = 2.5 μSv / h). Table 2 shows the beam lifetimes and dose equivalent rates as functions of straight section pressure. The maximum dose equivalent rate is obtained at $<P_L>$ = 1.33×10^{-3} Pa or 10^{-5} torr.

The upper limit on dose equivalent (r = 0.02 cm, depth = 29.5 cm) from gas bremsstrahlung in the unshielded case is approximately 3090 Sv. It would be

more appropriate to average the dose equivalent over a radius of 1 cm, (to represent exposure to an organ), in which case the upper limit in the unshielded case would be about 250 Sv. Since entry into the enclosures requires the closure of the safety shutters, one is exposed to the maximum dose equivalent only if the shutters fail to close. In this case, the exposure from synchrotron radiation will be much higher. The high dose equivalent rates encountered in the unshielded case promote the need for a fail-safe, redundant interlock system with high-reliability components. Individuals can also be exposed to doses of this magnitude outside the shielding if the safety stops are not in place at the back of the enclosures. Therefore it is of paramount importance to ensure that the safety stops are in place through the use of interlocks and/or and additional administrative measures.

Ion gauges and ion pumps in the storage ring will constantly monitor the vacuum in each sector of the ring. The stored beam will be aborted through the equipment protection system if the pressure in any sector reaches 0.133 to 1.33 mPa. However, for radiation protection purposes no credit is given for turning the beam off through the equipment protection system. It must be done through the Personnel Safety System.

6. Neutrons From Gas Bremsstrahlung

Neutrons may be produced in any target with which the gas bremsstrahlung interacts. These neutrons will have average energies of a few MeV. The neutron production depends on target material and dimensions, increasing with target thickness until it reaches a maximum, and then it saturates. The

neutron yields from infinitely thick targets are given as a function of energy in ref. [15].

Among the various elements for which neutron yields are given, tungsten has the second highest yield. Since both the FOE and WBH have tungsten gas bremsstrahlung safety stops, FLUKA was used to score the photon energy crossing the tungsten surface in the energy range of 6 MeV (~threshold for photo-neutron production) to 7 GeV. The maximum neutron yield from Swanson [15] was then used to determine the neutron dose equivalent rates outside the FOE/WBH. The dose equivalent rates outside the lateral wall (distance from safety stop = 1.2 m) and outside the back wall (distance from safety stop = 0.6 m) without accounting for transport/attenuation in the stop or the walls, are 6 and 16 μSv/h, respectively. Thus the tungsten stop will have to be shielded with about 15 cm of polyethylene (Tenth Value Layer = 13.0 cm for average energy = 2.0 MeV [16]) in the forward direction and 7 cm in the lateral direction in order to reduce the dose equivalent rates to less than 1.2 μSv/h.

Conclusions

Monte Carlo calculations indicate that the maximum value of the gas bremsstrahlung dose equivalent rate (for E_0 = 7 GeV, L = 15 m, I = 300 mA) in a 30-cm-thick tissue phantom occurs at a depth of 29.5 cm and is 2.1 Sv/h for a scoring area with radius = 0.02 cm. As the radius increases to 0.4 cm, the dose equivalent rate decreases to 0.57 Sv/h. These results were obtained with simulations performed at P_s = 1/10 atm for the straight section. Simulations at

Ps = 1/10 and 1 atm without suppression of multiple scattering underestimate dose equivalent when scored in areas with radii less than 2 cm. For simulations at Ps = 1 atm, the minimization of Bhabha and Moller scattering is important for scoring areas with radii less than 0.4 cm. The use of Rogers' fluence to dose equivalent conversion factors results in an overestimation of dose equivalent rates as expected.

The 18-cm-thick tungsten beam stop reduces the dose equivalent rate at a depth of 2.5 cm to 0.1 + 0.04 μSv/h when scored over an area with r = 1 cm. The corresponding dose equivalent rate with the tungsten stop is 32 mSv/h. After passing through the tungsten stop, the beam broadens due to the electromagnetic shower process. The tungsten stop has to be shielded with polyethylene to reduce the neutron dose equivalent rates outside the experimental enclosure to less than 1.2 μSv/h. The upper limit on the gas bremsstrahlung dose equivalent that an individual can be exposed to, outside the shielding, is 3.7 mSv for pressures in the straight section greater than the operating pressure.

Acknowledgments

The authors thank the various staff members of the APS Experimental Facilities, Alfredo Ferrari of INFN, Italy, and Ken Kase and Helmut Wiedmann of SLAC, for useful discussions and information. Gratitude is also expressed to the SLAC Publications Department for their help with this document.

References

[1] N. E. Ipe and A. Fassò, “Impact of Gas Bremsstrahlung on Synchrotron Radiation Beam Line Shielding at the Advanced Photon Source,” Proceedings of the 8th International Conference on Radiation Shielding, Arlington, Texas, April 24–28, 1994, SLAC–PUB–6410.

[2] A. Ferrari, M. Pelliccioni, and P. R. Sala, “Estimation of Fluence Rate and Absorbed Dose Rate Due to Gas Bremsstrahlung From Electron Storage Rings,” Nucl. Inst. Meth. B83, (1993) 518–524 .

[3] Radiological Control Manual, DOE N5480.6, US Department of Energy (June 1992).

[4] N. E. Ipe, D. R. Haeffner, E. E. Alp, S. C. Davey, R. J. Dejus, U. Hahn, B. Lai, K. J. Randall, and D. Shu, “Guide to Beam Line Radiation Shielding Design at the Advanced Photon Source,” ANL–APS–TB7 Argonne National Laboratory, Argonne, Illinois, (1993); SLAC–TN–93-5 (1993).

[5] A. Rindi, “Gas Bremsstrahlung from Electron Storage Rings,” Health Physics Vol. 42, No. 2, 187–193.

[6] A. Esposito and M. Pelliccioni, “Gas Bremsstrahlung Production in the Adone Storage Ring, LNF–86/23(NT), INFN, Frascati, Italy (1986).

[7] M. Pelliccioni and A. Esposito, “Measurements of Gas Bremsstrahlung in the Adone Storage Ring,” Proceedings of the 20th Midyear Topical Symposium of the Health Physics Society on Health Physics of Radiation Generating Machines, Reno, Nevada, Feb. 8–12, 1987, p. 495 .

[8] A. Rindi and G. Tromba, “Gas Bremsstrahlung from Bending Magnets,” ST / M–92 / 16, Sincrotrone Trieste, Trieste, Italy (1992).

[9] S. Ban, H. Hirayama, and S. Miura, “Estimation of Absorbed Dose due to Gas Bremsstrahlung From Electron Storage Rings,” Health Physics Vol. 57, No. 3, (1989) 407–412.

[10] J. C. Liu, W. R. Nelson, and K. R. Kase, “Gas Bremsstrahlung and Associated Photon-Neutron Shielding Calculations for Electron Storage Rings,” submitted to Health Physics, Stanford Linear Accelerator Center, Stanford, California (1994).

[11] A. Fassò, A. Ferrari, J. Ranft, P. R. Sala, G. R. Stevenson, and J. M. Zazula, “FLUKA 92,” presented at the Workshop on Simulating Radiation Environments, 11–15 January 1993, Santa Fe, New Mexico.

[12] P. A. Aarnio, A. Fassò, A Ferrari, J. H. Moehring, J. Ranft, P. R. Sala, G R. Stevenson, and J. M. Zazula, “Electron-Photon Transport: Always So Good as We Think? Experience with FLUKA,” Proceedings of the MC93 Conference, Tallahassee, Florida, 22–26 February 1993.

[13] J. E. Turner, H. A. Wright, and R. N. Hamm, “Review Article, A Monte Carlo Primer for Health Physics,” Health Physics Vol. 48, No. 6, (1985) 717–733.

[14] D. W. O. Rogers, “Fluence to Dose Equivalent Conversion Factors Calculated With EGS3 for Electrons From 100 keV to 20 GeV and Photons From 11 keV to 20 GeV,” Health Physics Vol. 46, No. 4, pp. 891–914 (1984).

[15] International Atomic Energy Agency, Radiological Safety Aspects of the Operation of Electron Linear Accelerators, Technical Report Series No. 188 (written by W. P. Swanson), IAEA, Vienna (1979).

[16] NCRP, Neutron Contamination from Medical Electron Accelerators, NCRP No. 79, National Council on Radiation Protection and Measurements, (Bethesda, Maryland) (1984).

Figures

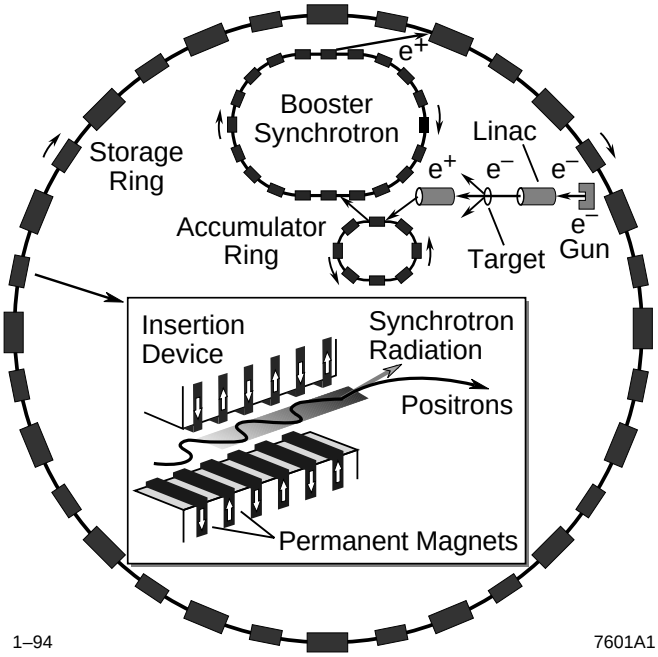

Figure 1. The Advanced Photon Source.

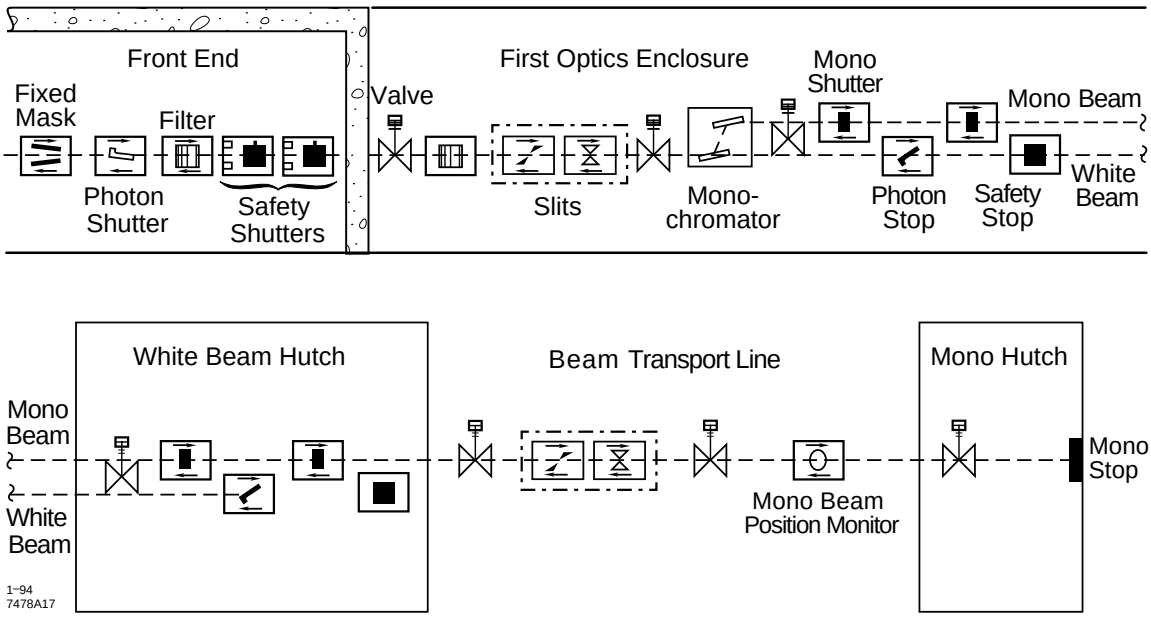

Figure 2. Schematic of a model APS SR beam line.

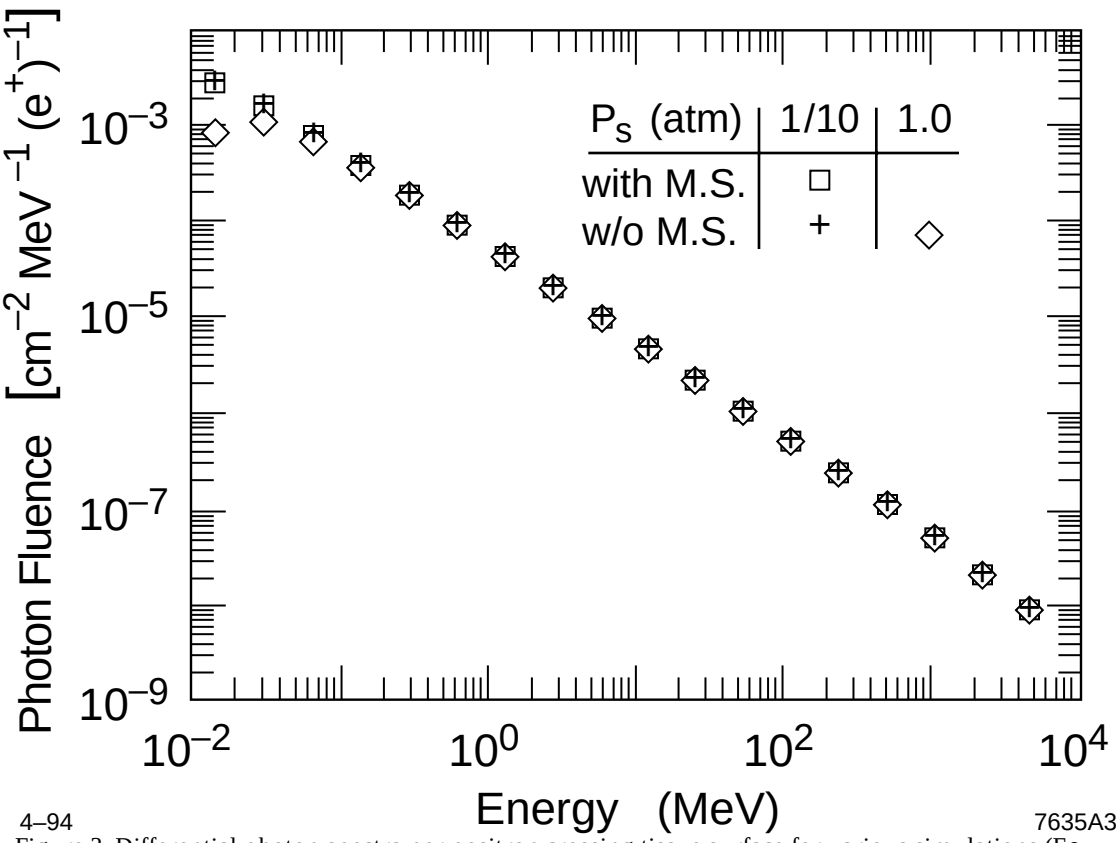

Figure 3. Differential photon spectra per positron crossing tissue surface for various simulations (E_0 = 7 GeV, P = 1 atm, L = 15 m, AE for air target = 10 keV, r = 20 cm).

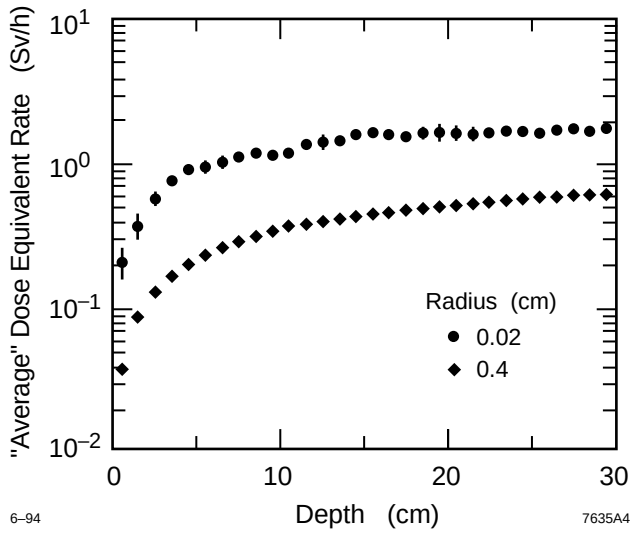

Figure 4. “Average” dose equivalent rate as a function of depth in tissue for different radii (E_0 = 7 GeV, P = 0.133 μPa, P_S = 1 / 10 atm, L = 15 m, I = 300 mA, AE for air target = 10 keV).

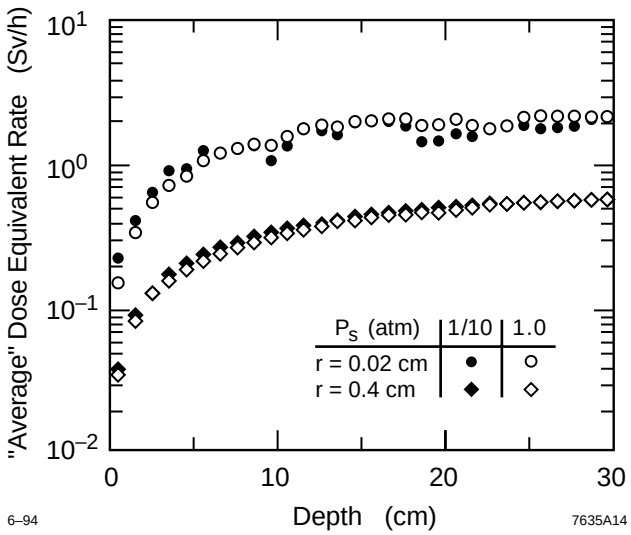

Figure 5 “Average” dose equivalent rate as a function of depth in tissue for different radii (E_0 = 7 GeV, P = 0.133 μPa, L = 15 m, I = 300 mA, AE for air target = 10 MeV).

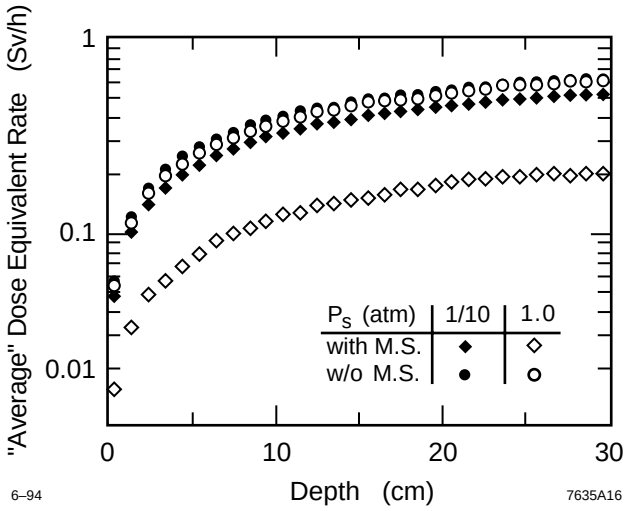

Figure 6 “Average‘‘ dose equivalent rate as a function of depth in tissue for various simulations (E_0 = 7 GeV, P = 0.133 μPa, I = 300 mA, L = 15 m, AE for air target = 10 MeV, r = 0.4 cm).

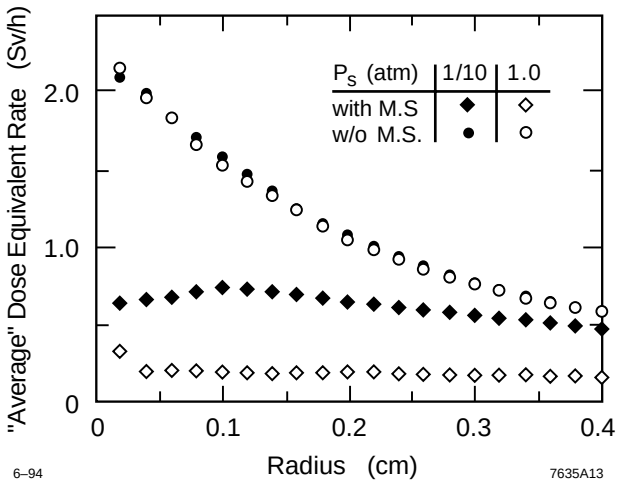

Figure 7. "Average" dose equivalent rate as a function of radius (0–0.4 cm) in tissue for various simulations (E_0 = 7 GeV, P = 0.133 μPa, I = 300 mA, L = 15 m, AE for air target = 10 MeV, depth = 29.5 cm).

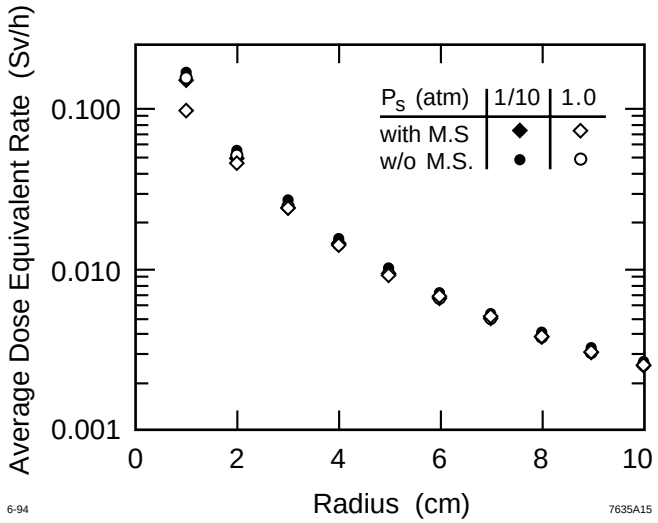

Figure 8 "Average" dose equivalent rate as a function of radius (0–20 cm) in tissue for various simulations (E_0 = 7 GeV, P = 0.133 μPa, I = 300 mA, L = 15 m, AE for air target = 10 MeV, depth = 29.5 cm).

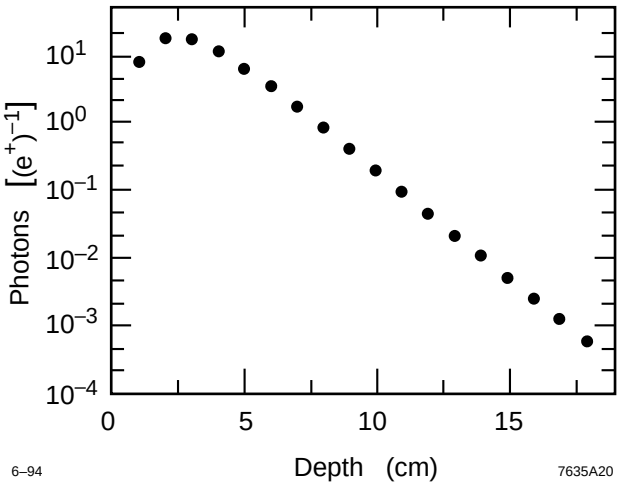

Figure 9. Number of photons per positron crossing various depths in tungsten beam stop (E_0 = 7 GeV, P = 1 atm, Ps = 1/10 atm, L = 15 m, AE for air target = 10 MeV, r = 10 cm).

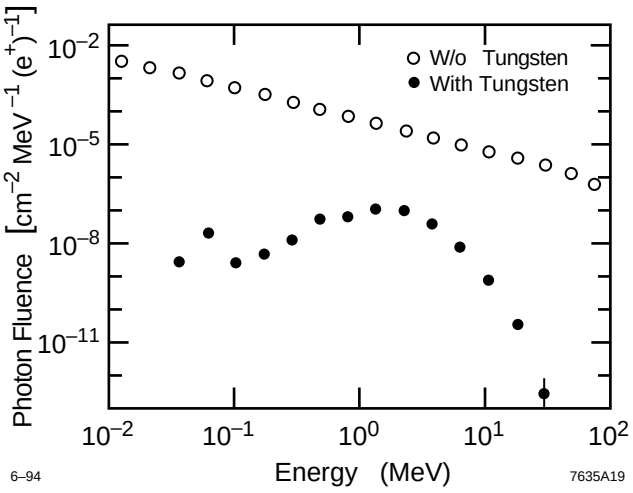

Figure 10. Differential photon spectra per positron crossing tissue surface with and without tungsten stop (E_0 = 7 GeV, P = 1 atm, Ps = 1/10 atm, L = 15 m, AE for air target = 10 MeV, r = 20 cm).

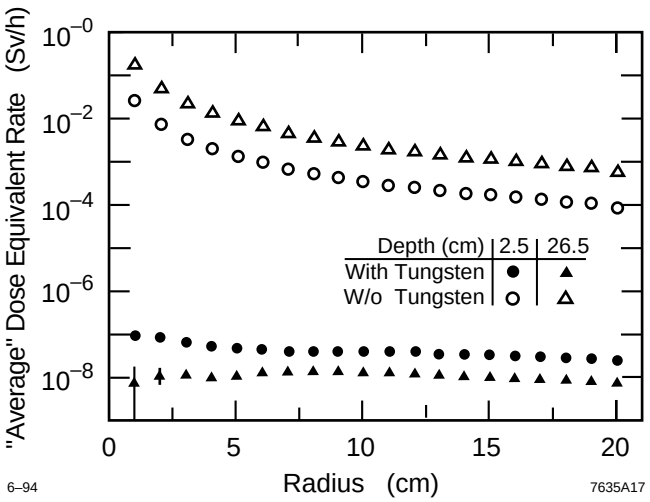

Figure 11. “Average” dose equivalent rate as a function of radius in tissue at different depths, with and without tungsten stop (E_0 = 7 GeV, P = 0.133 μPa, I = 300 mA, Ps = 1/10 atm, L = 15 m, AE for air target = 10 MeV).

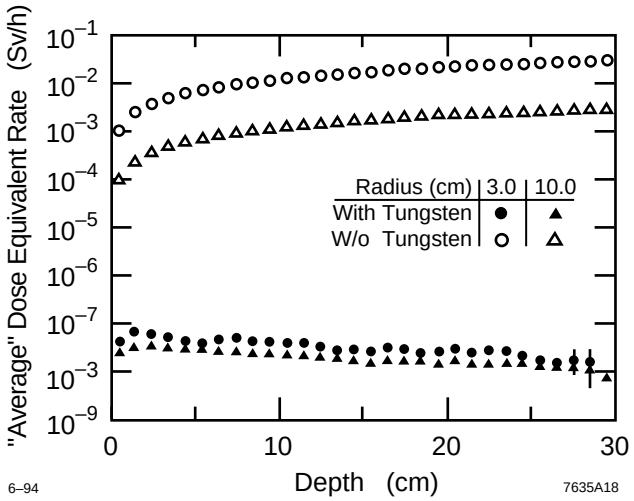

Figure 12. “Average” dose equivalent rate as a function of depth in tissue for different radii with and without tungsten stop (E_0 = 7 GeV, P = 0.133 μPa, Ps = 1 atm, I = 300 mA, L = 15 m, AE for air target = 10 MeV).

Tables

	APS	ESRF	SSRL
E_0(GeV)	7.0	6.0	3.0
I (mA)	300	100	100
L (m)	15	15	5
d (m)	20	20	20
Dose Rate Ratio	61	14	1

1–94 7478A18

Table 1. Ratio of gas bremsstrahlung dose rates at various SR facilities.

$\langle P_L \rangle$ (Pa)	τ (h)	Dose Equivalent (Sv)
1.33×10^{-7}	20	5×10^{-5}
1.33×10^{-6}	17.8	4.5×10^{-4}
1.33×10^{-5}	8.5	2.1×10^{-3}
1.33×10^{-4}	1.37	3.4×10^{-3}
1.33×10^{-3}	0.15	3.7×10^{-3}

5–94 7501A11

Table 2. Beam lifetimes and dose equivalent rates as a function of straight section pressure.